Journal of Metals, Materials and Minerals, Vol. 29, No. 3, pp. 82-87, 2019

Incorporating black dust into autoclaved aerated concrete wall for heat transfer reduction

Somchai MANEEWAN[1], Ketwadee JANYOOSUK[1], Chan HOY-YEN[2], and Atthakorn THONGTHA[1,*]

[1] *Department of Physics, Faculty of Science, Naresuan University, Phitsanulok, 65000, Thailand*
[2] *Solar Energy Research Institute, Universiti Kebangsaan Malaysia, Kuala Lumpur, 50566, Malaysia*

[*]**Corresponding author e-mail:** atthakornt@nu.ac.th

Received date:
30 September 2018
Revised date:
22 January 2019
Accepted date:
27 January 2019

Keywords:
Black dust
Autoclaved aerated concrete
Heat transfer reduction
Automotive refinishing industry

Abstract

Black dust is a waste product of the automotive refinishing industry in Thailand. Instead of removing black dust by landfill disposal, an innovative approach of utilizing black dust as the mixture for the preparation of autoclaved aerated concrete (AAC) was investigated. Results demonstrate that black dust is able to provide higher compressive strength and more extended time lag than conventional materials. The chemical properties of black dust were investigated by using X-ray fluorescence analyzer. The use of black dust content of 20 wt.% replacement of fine sand was the optimum composition, which possessed a low density of around 0.58 $g \cdot cm^{-3}$, a maximum compressive strength of ~ 4.6 MPa and the lowest proportion of thermal conductivity of 0.120 $W \cdot m^{-1}K^{-1}$. The AAC incorporating the optimum black dust content significantly increased in the thermal effectiveness of the building materials by extending approximately 25% the time for the heat wave to flow through the exterior wall to the interior wall, reducing ~ 33% heat flux and achieving ~ 4.7% lower room temperature when compared with the conventional AAC.

1. Introduction

The commercial and residential buildings consumed ~35% of the world energy demand [1]. Thus, reducing energy consumption in buildings is crucial to ensure a sustainable low carbon living. One of the solutions is through the buildings wall thermal insulation. Nonetheless, conventional insulation of walls has less significant in reducing cooling loads in hot and humid climates, and may trap heat inside the buildings. On the other hand, autoclaved aerated concrete (AAC), which has low thermal conductivity and high heat resistant, is able to serve as the building wall and simultaneously as an insulation without an additional insulation layer.

AAC is commonly used in building applications such as wall panels, masonry blocks, roof decks, and precast concrete units. It is a lightweight concrete that has an approximate porosity of 80%, lower shrinkage, lower thermal conductivity, easier and faster in construction process compared to the conventional concrete [1-3, 5, 6]. Furthermore, research found that this material is able to achieve an energy saving up to 50% [4].

Utilising the industrial by-products and recycling the wastes to be used as part of the raw materials for preparing the AAC have been extensively investigated. Such recycled wastes were from efflorescence sand and phosphorus slag [7], iron ore tailings [8], air-cooled slag [9], siliceous crushed stone [10], lead–zinc tailings [11], coal bottom ash [12], copper tailings and blast furnace slag [13] and calcium fly ash and natural zeolite [14].

Large amounts of black dust waste are globally generated during the process of automotive production in the part of the polishing processes of automotive industry and created a great problem on environmental and human impacts in each year, particularly in the landfill phase of disposal. Thailand is one of the important automotive industry countries that ranked 12th in the world [15]. Thus, the availability of black dust is abundant in Thailand. Instead of treating black dust to the landfill disposal, black dust can be used as raw materials to produce the AAC. Therefore, this present work is to replace the fine sands content with the black dust, which has not yet previously investigated. The effects on the compressive strength, thermal conductivity and decrement factors of AAC were studied, and heat transfer from the exterior to the interior walls was also examined.

2. Experimental methodology

2.1 Raw materials and preparation of AAC

The commercially available raw materials in preparing the AAC preparation are aluminum (Al), anhydrite ($CaSO_4$), lime (CaO), Portland cement and fine sand (less than 90 μm in size). While the concrete mix was prepared according to the mixture composition of AAC

DOI: 10.14456/jmmm.2019.39

by percent of weight, i.e. 0.06 wt.% of aluminum, 1.64 wt.% of anhydrite, 11.94 wt.% of lime, 12.43 wt.% of Portland cement and 73.93 wt.% of fine sand.

The chemical compositions of sand and black dust waste were characterized by X-ray fluorescence (XRF). The values of percent by weight of the replacement of fine sand by using black dust (identified as AAC-BD) are 0%, 15%, 20%, 25%, 30%, 35%, 40%, 45% and 50%. All compositions of AAC were well-incorporated with water in a mold size of 20cm × 20cm × 100cm, were then prepared at temperature of 180-190°C and the pressure of 12 bars from a manufacturer that has been certified by Thailand Industrial Standard (TIS) 1505-1998.

2.2 Compressive strength, density and thermal conductivity measurement

After the autoclave process, the AAC-BD samples were cut into uniform blocks in dimension of 7.5cm×7.5cm×7.5cm. The AAC-BD samples were then tested for the dry density, water absorption and the compressive strength. For the compressive strength test, in accordance with the ASTM C1555-03a, some of these blocks were dried at 75°C for 24 h. For the density test, according to the ASTM C642-97 standards, samples were dried at 105°C for 24 h. The thermal conductivity tester was used to determine the thermal conductivity for the AAC-BD samples.

2.3 Testing room design and air temperature measurements

Two small rooms were used to study the thermal effectiveness performance, which each room was 0.288 m^3 in volume (Figure 1). These rooms were constructed using the wooden wall which was insulated by polyetylene sheets. For each room, the south-facing walls were constructed with the original AAC and the optimal AAC-BD composition wall materials respectively.

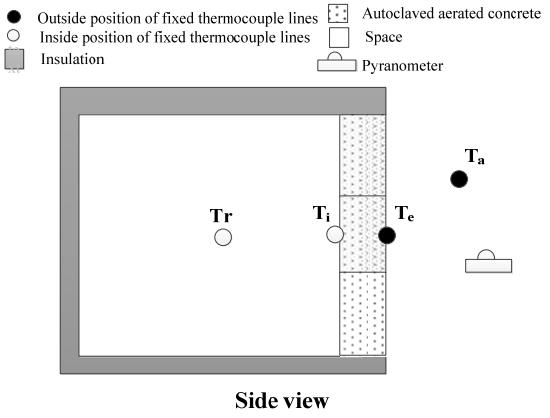

Figure 1. Thermal couples positions for the testing set up.

The exterior and interior wall surfaces temperature, room temperature and ambient temperature were measured by using K-type thermocouples with ± 0.5°C accuracy as illustrated in Figure 1. At positions of the outer and inner wall surfaces, the thermocouples were covered with aluminum foil tape. Kipp and Zonen solarimeter (accuracy ± 2%) was used to test the solar radiation intensity incident on a horizontal plane. Wind anemometer was used to measure the wind speed. In real ambient condition, all data were saved at 5 min interval and continuously recorded over 24 h using a data logger. Time lag and decrement factors were also studied in real ambient condition.

3. Results and discussion

3.1 Chemical analysis

Table 1 shows the main oxide chemical compositions of sand and black dust samples. This showed the similarity of the chemical composition between black dust and fine sand. Fine sand was appropriately replaced by using the black dust waste. The substitution of sand content in the normal autoclaved aerated concrete mixture was confirmed that it did not affect to the overall chemical composition of AAC mixture and any chemical change in other materials in the concrete mixture. The other raw materials contents were therefore fixed, and black dust waste was only replaced into the sand. This study concentrated on the replacement of sand content by black dust waste to obtain the outstanding composition of AAC and to fabricate the excellent compressive strength obtainable.

Table 1. Chemical composition of fine sand and black dust.

Main oxide composition	Fine sand (%)	Black dust (%)
SiO_2	86.70	64.55
Al_2O_3	6.85	23.36
Fe_2O_3	1.10	4.54
CaO	0.45	2.24
MgO	0.87	0.95
Na_2O	1.20	0.31
K_2O	0.90	1.21

3.2 Compressive strength

The compressive strength of autoclaved aerated concrete with different contents of black dust is shown in Figure 2. The value of the compressive strength of the AAC-BD initially increased and reached its maximum strength with the black dust content of 20 wt.% and afterwards decreased when the content of black dust was more added. The highest compressive strength was at ~4.6 $N \cdot mm^{-2}$ at AAC samples with the content of the 20 wt.% black dust. This value is higher

than all other concrete mixtures that consisted of coal bottom ash (2.78 $N \cdot mm^{-2}$) [12], copper tailings and blast furnace slag (4.00 $N \cdot mm^{-2}$) [13] and high-calcium fly ash and natural zeolite (4.51 $N \cdot mm^{-2}$) [14]. Therefore, this highest compressive strength (4.6 $N \cdot mm^{-2}$) of the content of the 20 wt.% black dust is around 15% higher than the AAC without black dust and is between 2% and 66% greater than the maximum value received by utilizing other industrial waste products [12-14].

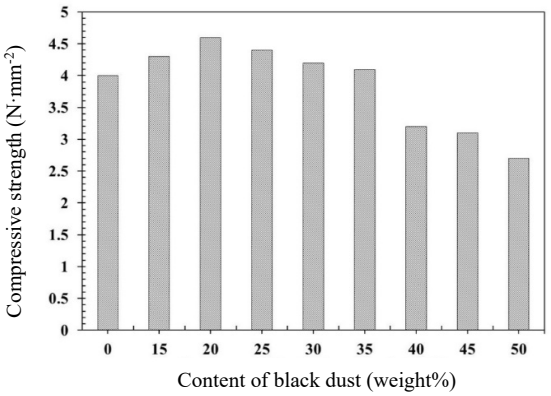

Figure 2. The compressive strength of AAC with the variation between fine sand and black dust.

3.3 Density, water absorption and thermal conductivity

The density and water absorption of AAC-BD with various contents of black dust are displayed in Table 2. When there was an increase of black dust contents from 0% to 50 % by weight, the density reduced from 0.60 to 0.54 $g \cdot cm^{-3}$, while the water absorption slightly increased from 0.39 to 0.43 $g \cdot cm^{-3}$. This was observed that the optimum composition was found at the samples with the black dust content of 20 wt.% because of showing its maximum compressive strength. The density of this composition was claimed in quality class of 4 (0.51–0.80 $g \cdot cm^{-3}$) and the water absorption was also in quality class of 4 ($\leq$0.50 $g \cdot cm^{-3}$), which are also based on the Thai Industrial Standard 1505-1998. Of more significance, the thermal conductivity of AAC-BD decrease from 0.157 to 0.125 $W \cdot m^{-1} \cdot C^{-1}$ with an increasing of the black dust content from 0% to 50% by weight as exhibited in Table 2. A decrease of the thermal conductivity corresponded to a decrease of density because lower density is related to more air void that efficiently prevent the thermal transmission. Incorporating black dust as the mixture for the preparation of autoclaved aerated concrete demonstrated the better insulating properties that lead to a reduction of heat transfer. Importantly, this result causes an energy saving in buildings and a significant reduction of the yearly highest cooling demand.

To investigate the thermal performance of the ordinary AAC and the optimum AAC-BD (AAC with the black dust content of 20 wt.%), the two small testing rooms with different wall materials were tested. Figure 3-5 show the result from the test rooms with different wall types that measured concurrently. The external and internal surface temperature evolution and room temperature of the two rooms were investigated and compared.

3.4 Exterior and interior surface temperature evolution of house wall

The evolutions of solar radiation, ambient temperature and exterior and interior wall surface temperature in the south side are shown in Figure 3. This study was tested and noted from 6 am of day to 6 am of the following day, giving a 24 h test cycle. The nature evolution of solar radiation in the tropic due to periodical cloud cover that is normal between sunrise (6.00 am) and sunset (6.00 pm) with the maximum value of around 900 $W \cdot m^{-2}$ around midday. Wind velocity in the testing area was between 0.20 and 3.50 $m \cdot s^{-1}$. The ambient temperature fluctuated between ~27°C in the morning between 5-6 am and up the maximum value of ~37°C at around midday.

Table 2. Density, water absorption and thermal conductivity of AAC with various contents of black dust.

Content of black dust (weight%)	Density ($g \cdot cm^{-3}$)	Water absorption ($g \cdot cm^{-3}$)	Thermal conductivity ($W \cdot m^{-1}K^{-1}$)
0	0.60	0.39	0.157
15	0.57	0.40	0.148
20	0.58	0.40	0.140
25	0.57	0.41	0.142
30	0.58	0.40	0.138
35	0.58	0.40	0.134
40	0.56	0.42	0.132
45	0.54	0.43	0.128
50	0.54	0.43	0.125

Considering the AAC room, the temperature evolutions of the exterior surfaces of the south side are illustrated as Figure 3 (a). The maximum exterior AAC wall temperature reached as high as ~55.6°C at about midday. For the AAC-BD room, the temperature evolutions of the exterior surfaces of the south side are also shown as Figure 3 (a). The maximum exterior AAC-BD wall temperature peaked as high as ~51.6°C at around midday.

Considering the AAC room, the temperature evolutions of the interior surfaces of the south side are displayed as Figure 3 (b). The maximum internal AAC wall temperature arrived as high as about 44.7°C at around 2 pm. For the AAC-BD room, the temperature evolutions of the interior surfaces are also exhibited as Figure 3 (b). The maximum interior AAC-BD wall temperature reached as high as ~42.2°C at around 2.30 pm.

This is observed that the AAC-BD wall temperature fluctuations are lower than for the ordinary AAC walls. The temperature evolution curves between AAC-BD and ordinary AAC walls have a phase difference of around 30 min. Therefore, this is presumed that sand replacement by the black dust waste in the optimum condition produces AAC with the inertia is higher than the ordinary AAC wall. Concerning the interior wall temperature curve, the AAC-BD material causes a reduction of the temperature amplitude of about 2.5ºC.

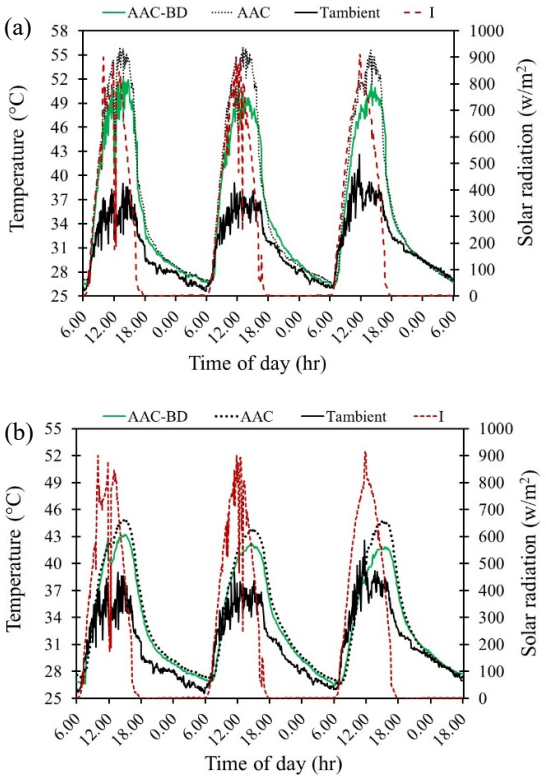

Figure 3. Comparison of (a) exterior and (b) interior wall temperatures of the two testing rooms.

3.5. Comparison of flux evolution

Figure 4 shows the heat fluxes of the internal and external wall surfaces of the traditional AAC wall and the AAC-BD wall (AAC with incorporating the optimum black dust content). As the heat transfer from the exterior surface to the interior surface, heat flux on the wall is positive (The temperature of inner surface is lower than that of outer surface), while the heat transfers from the interior surface to the exterior surface, heat flux on the wall is negative (The temperature of inner surface is higher than that of outer surface).

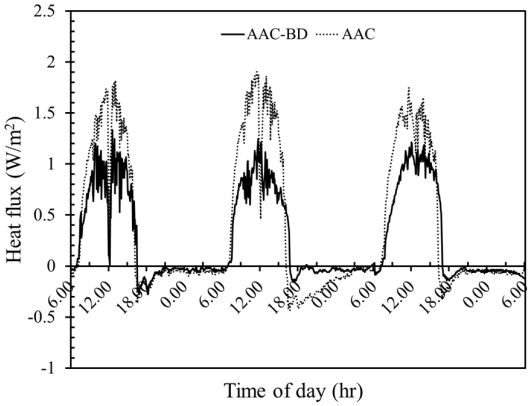

Figure 4. Comparison of heat flux evolution of the two rooms.

With the heat fluxes of the AAC house wall, positive heat flux of the south surfaces was initially increased and arrived to its highest value of about 1.8 $W \cdot m^{-2}$ at around midday and then dropped in value over time passed after each those times. It was found that the negative heat fluxes of the south surfaces began at about 5.00 pm. The highest value of the heat fluxes was about 0.4 $W \cdot m^{-2}$ at around 6.00 pm, afterwards dropped for day time below these values.

For the heat fluxes of AAC-BD wall, the maximum positive value of the south surfaces was observed at about 1.2 $W \cdot m^{-2}$ at around midday. The maximum negative value of the south surfaces was observed at about 0.2 $W \cdot m^{-2}$ at about 6.00 pm. This result shows the maximum positive heat flux of the AAC-BD wall was less than that of the AAC wall of ~0.6 $W \cdot m^{-2}$. This demonstrates that the sand replacement by the black dust waste in the optimum condition can decrease the heat transfer through the building wall and result in a development in the insulative efficiency of buildings. This is clearly a significant result.

3.6. Comparison of room temperature

Figure 5 exhibits the room temperature of the two testing rooms with different wall types between 6 am of day and 6 am of the following day. The evolution of solar radiation, ambient temperature, and outer and

inner surface temperature of the house walls result in the fluctuation of room temperature in each one through the period of the day. It was observed that the room temperature of the two rooms was approximately equal between the times of 6 am and 11.30 am. After that time, different peak temperatures were reached in each test house at different times. After 11.40 am the temperature readings diverged. The room temperature of the AAC house rose more rapidly, and achieved the highest peak value of around 42.6°C at about 2.30 pm. The room temperature of the AAC-BD room peaked at 40.6°C at about 3 pm. The optimum composition of sand replacement by black dust enables to maintain the room temperature within the comfort zone by decreasing the maximum room temperature to a maximum value of 2.0°C. This clearly demonstrated that the peak difference of AAC-BD room temperature was more extended than that of ordinary AAC temperature for 30 min, which indicated the greater insulative efficiency of AAC consisting of black dust.

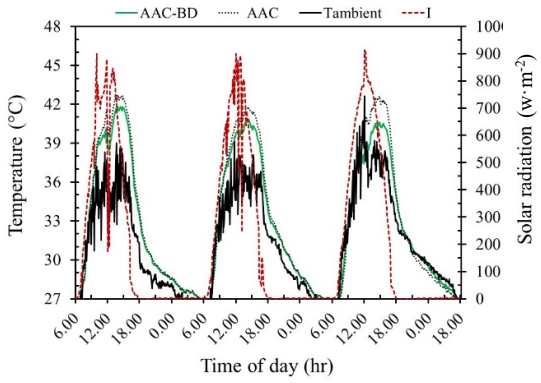

Figure 5. Comparison of room temperature of the two rooms.

3.7 Time lag and decrement factor

The thermal performance of traditional AAC and AAC-BD wall was evaluated by time lag (ϕ) and the decrement factor (*f*) [16-17]. The time lag is the time that the dynamics of heat through the exterior wall to the interior wall. The decrement factor is the reducing proportion of temperature fluctuation [16-17]. The heat flux time lag and decrement factor are therefore determined as shown in the equations (1) and (2).

$$\Phi = \tau_{qi,max} - \tau_{qe,max} \quad (1)$$

$$f = \frac{A_i}{A_e} = \frac{q_{i,max} - q_{i,min}}{q_{e,max} - q_{e,min}} \quad (2)$$

Where $\tau_{qi,max}$, $\tau_{qe,max}$ are the times at the peak of interior and exterior wall heat flux. A_i and A_e are the amplitudes of heat wave of inner and outer wall surfaces. $q_{i,max}$, $q_{i,min}$, $q_{e,max}$, $q_{e,min}$ are the highest and lowest heat wave of the internal and external wall surface, respectively.

For the ordinary AAC, the time lag and decrement factor were at around 120 min and 0.6. For the AAC-BD, the time lag and the decrement factor were at approximately 150 min and 0.5. This shows that the time lag of AAC-BD was slightly more extended than that of AAC. The decrement factor of AAC-BD was slightly lower than that of ordinary AAC as well. This indicated that the sand replacement by black dust in the optimum ratio can slightly expand the time of thermal inertia to transfer through the exterior wall surface to the interior wall surface and certainly reduce the amplitude proportion during this process, which demonstrate an ~2°C lower room temperature of AAC-BD with comparing that of the ordinary AAC.

4. Conclusions

This is the first paper discusses an AAC block is successfully prepared by using black dust waste. It is found that the black dust content of 20 wt.% for sand replacement is the optimum composition with the highest compressive strength of 4.6 $N \cdot mm^{-2}$. This compressive strength value is between 2% and 66% higher than the other conventional AACs. And the most importantly, the sand replacement by black dust in the optimum mixture is able to reduce the heat transfer from the exterior wall surface to the interior wall surface and hence the internal room spaces. The AAC-BD wall is able to reduce ~33% of heat flux and 4.7% of room temperature compared to the conventional AAC wall. Therefore, the AAC-BD is suitable to be applied as an adjunct material to replace the traditional concrete for non-structural (non-load bearing) walls and masonry constructions in the future.

5. Acknowledgements

The authors would like to thank the Thailand Research Fund (TRF), Faculty of Science, Naresuan University and INSEE Superblock Company Limited, and the National University of Malaysia (GUP-2015-035) for providing financial support to this research work, and our research center.

References

[1] L. J. Hunag, H. Y. Wang, and Y. W. Wu, "Properties of the mechanical in controlled low-strength rubber lightweight aggregate concrete (CLSRLC)," *Construction and Building Materials*, vol. 112, pp. 1054-1058, 2016.

[2] A. Wongsa, Y. Zaetang, V. Sata, and P. Chindaprasirt, "Properties of lightweight fly ash geopolymer concrete containing bottom ash as aggregates," *Construction and Building Materials*, vol. 111, pp. 637-643, 2016.

[3] N. Dulsang, P. Kasemsiri, P. Posi, S. Hiziroglu, and P. Chindaprasirt, "Characterization of an environment friendly lightweight concrete containing ethyl vinyl acetate waste," *Materials & Design*, vol. 96, pp. 350-356, 2016.

[4] H. S. Tao, *Research for developing aerated concrete by using fly ash with high calcium of Gehua power plant in Hongshan*, Wuhan University of Technology, WuHan, 2004.

[5] O. Koronthalyova, "Moisture storage capacity and microstructure of ceramic brick and autoclaved aerated concrete," *Construction and Building Materials,* vol. 25, pp. 879-885, 2011.

[6] I. B. Topcu and B. Isıkdag, "Effect of expanded perlite aggregate on the properties of lightweight concrete," *Journal of Materials Processing Technology*, vol. 204, pp. 34-38, 2008.

[7] B. G. Ma and X. Zheng, "Study on a new kind of aerated concrete containing efflorescence sand-phosphorus slag–lime," *Journal of Building Materials*, vol. 2, no. 3, pp. 223-228, 1999.

[8] Y. Wang, J. Yin, J. C. Chen, and C. Q. Peng, "Aerocrete made with low silicon tailings of Cheng Chao iron ore mine," *Journal Wuhan University of Technology, Materials Science Edition*, vol. 15, no. 2, pp. 58-62, 2000.

[9] N. Y. Mostafa, "Influence of air-cooled slag on physicochemical properties of autoclaved aerated concrete," *Cement and Concrete Research*, vol. 35, pp. 1349-1357, 2005.

[10] Q. K. Wang, Y. Z. Chen, F. X. Li, T. Sun, and B. B. Xu, "Microstructure and properties of silty siliceous crushed stone-lime aerated concrete," *Journal Wuhan University of Technology, Materials Science Edition*, vol. 21, no. 2, pp. 17-20, 2006.

[11] F. X. Li, Y. Z. Chen, and S. Z. Long, "Experimental investigation on aerated concrete with addition of lead–zinc tailings," *Journal of Southwest Jiaotong University*, vol. 43, no. 6, pp. 810-815, 2008.

[12] H. Kurama, I. B. Topcu, and C. Karakurt, "Properties of the autoclaved aerated concrete produced from coal bottom ash," *Journal of Materials Processing Technology*, vol. 209, pp. 767-773, 2009.

[13] X. Y. Huang, W. Ni, W. H. Cui, Z. J. Wang, and L. P. Zhu, "Preparation of autoclaved aerated concrete using copper tailings and blast furnace slag," *Construction and Building Materials*, vol. 27, pp. 1-5, 2012.

[14] K. Jitchaiyaphum, T. Sinsiri, C. Jaturapitakkul, and P. Chindaprasirt, "Cellular lightweight concrete containing high-calcium fly ash and natural zeolite," *International Journal of Minerals, Metallurgy and Materials*, vol. 20, no. 5, pp. 462-471, 2013.

[15] International Organization of Motor Vehicle Manufacturers, 2017. 2017 Production statistics, Available from: http://www.oica.net/category/production-statistics/2016-statistics/

[16] A. Thongtha, A. Khongthon, T. Boonsri, and H. Y. Chan, "Thermal effectiveness enhancement of autoclaved aerated concrete wall with PCM-contained conical holes to reduce the cooling load," *Materials*, vol. 12, no. 13, pp. 2170, 2019.

[17] A. Thongtha, S. Maneewan, C. Punlek, and Y. Ungkoon, "Investigation of the compressive strength, time lags and decrement factors of AAC-lightweight concrete containing sugar sediment waste," *Energy and Buildings*, vol. 84, pp. 516-525, 2014.